



Peculiarities of Wave Fields in Nonlocal Media

V.A. Danylenko and S.I. Skurativskyi *

Division of Geodynamics of Explosion, Subbotin Institute of Geophysics, National Academy of Sciences of Ukraine, Bohdan Khmelnytskyi Str. 63 B, 01054, Kyiv-54, Ukraine

Received: May 12, 2015; Revised: March 29, 2016

Abstract: The paper summarizes the studies of wave fields in structured non-equilibrium media described by means of nonlocal hydrodynamic models. Due to the symmetry properties of models, we derived the invariant wave solutions satisfying autonomous dynamical systems. Using the methods of numerical and qualitative analysis, we have shown that these systems possess periodic, multiperiodic, quasiperiodic, chaotic, and soliton-like solutions. Bifurcation phenomena caused by the variation of nonlinearity and nonlocality degree are investigated as well.

Keywords: *nonlocal models of structured media; travelling wave solutions; chaotic attractor; homoclinic curve; invariant tori.*

Mathematics Subject Classification (2010): 74D10, 74D30, 37G20, 34A45.

1 Introduction

Open thermodynamic systems attract attention of scientists by their synergetic properties, their ability to produce localized nontrivial structures and order. Description of such phenomena requires the creation of new and the refinement of already known mathematical models.

According to [1–3], with the methods of non-equilibrium thermodynamics and the internal variables concept [6], the nonlinear temporally and spatially nonlocal mathematical models have been constructed for non-equilibrium processes in media with structure. In

* Corresponding author: <mailto:skurserg@rambler.ru>

this paper, we present the results of investigations of wave processes in such media. To this end, we use the following hydrodynamic type system

$$\begin{aligned} \dot{\rho} + \rho u_x = 0, \quad \rho \dot{u} + p_x = \gamma \rho^m, \\ \frac{1}{\rho^2} \frac{\Gamma \varepsilon_r}{\tau_{TP}} \left\{ \left[-\rho_{xx} (1 + \mathbf{a}) + \frac{1}{\rho} (\rho_x)^2 (1 - \mathbf{a} \Gamma_{V0}) \right] + [-\ddot{\rho} (1 + \mathbf{a}) + \right. \\ \left. + \frac{2}{\rho} \dot{\rho}^2 \left(1 - \frac{\mathbf{a} (\Gamma_{V0} - 1)}{2} \right) + \frac{1}{\tau_{TP}} \dot{\rho} (1 + \mathbf{a}) \right] \} + \omega_0^2 \rho_0^{1 - \Gamma_{V0}} \rho^{\Gamma_{V0}} \\ - \omega_0^2 \rho_0 = b (p - p_0) + b \tau_{TV} \dot{p} - \frac{\chi T_0}{\chi T_\infty} b \tau_{TV}^2 \ddot{p} - b \Gamma \varepsilon_r \tau_{TV} \left(p_{xx} + \frac{\rho_x}{\rho} p_x \right), \end{aligned} \quad (1)$$

where

$$\mathbf{a} = T_0 \alpha_\infty \Gamma_{V0} \left(\frac{\rho}{\rho_0} \right)^{\Gamma_{V0} + 1}, \quad \omega_0^2 = \frac{b c_{S0}^2 \alpha_0 T_0}{\gamma_0}, \quad b = \frac{\chi T_0}{\rho_0 \tau_{TP}^2}, \quad \chi T_0 = \rho_0^{-1} c_{T0}^{-2} = \gamma_\infty \rho_0^{-1} c_{S0}^{-2};$$

c_{T0} , c_{S0} are the isothermal and adiabatic frozen velocities of sound; γ_∞ is the frozen polytropic index, $\gamma \rho^m$ is the mass force.

Using the characteristic quantities t_0 , u_0 , ρ_0 , let us construct the scale transformation

$$\begin{aligned} t = \bar{t} t_0, \quad x = \bar{x} t_0 u_0, \quad p = \bar{p} \rho_0 u_0^2, \quad \rho = \bar{\rho} \rho_0, \quad u = \bar{u} u_0, \\ \sigma = \frac{\Gamma \varepsilon_r \tau_{TV}}{(t_0 u_0)^2}, \quad \tau_{pT} = \tau_{TV} \frac{\chi T_0}{\chi T_\infty}, \quad \tau = \frac{\tau_{TV}}{t_0}, \\ h = \frac{\chi T_0}{\chi T_\infty} \tau^2, \quad \kappa = \frac{\omega_0^2}{b u_0^2}, \quad \chi = \frac{1}{\rho_0 u_0^2 \chi T_\infty}, \quad a = \delta n \rho^{n+1}, \quad \delta = T_0 \alpha_\infty, \quad \Gamma_{V0} = n, \end{aligned} \quad (2)$$

which leads system (1) to the dimensionless form

$$\begin{aligned} \dot{\rho} + \rho u_x = 0, \quad \rho \dot{u} + p_x = \gamma \rho^m, \\ \sigma \chi \rho^{-2} \left[-\rho_{xx} (1 + a) + \rho_x^2 \rho^{-1} (1 - a n) \right] + h \chi \rho^{-2} \\ \left[-\ddot{\rho} (1 + a) + 2 \dot{\rho}^2 \rho^{-1} (1 - 0.5 a (n - 1)) + \tau h^{-1} \dot{\rho} (1 + a) \right] \\ + \kappa \rho^n = p + \tau \dot{p} - h \ddot{p} - \sigma (p_{xx} + \rho_x p_x \rho^{-1}). \end{aligned} \quad (3)$$

We would like to emphasize that system (3) can be regarded as a hierarchical set of submodels which are complicated by taking new effects into account. We are thus going to study the chain of nested models and to classify their wave solutions using the methods of qualitative and numerical analysis.

The remainder of the paper is organized as follows. In Section 2 we begin our studies with a simplified version of system (3) keeping the terms with the first temporal derivatives, then attaching the terms with the second temporal or spatial derivatives. The form of wave solutions and the description of techniques for their exploration are presented in detail. Section 3 is devoted to the spatially nonlocal model which is used for investigating the Shilnikov homoclinic structures whose existence and bifurcations are extremely important during chaotic regimes formation. The model incorporating both temporal and spatial nonlocalities is presented in Section 4. Generalizations of the previous models by means of introducing the third temporal derivatives and incorporating physical nonlinearity are given in Section 5 and Section 6, respectively. For all models we derive invariant wave solutions and carry out the qualitative analysis of the corresponding factor-systems.

2 Wave Solutions of the Models with Dynamic Equation of State (DES) Incorporating the Second Temporal or Spatial Derivatives

To begin with, let us consider the simplest model with relaxation derived from (3) at $\delta = h = \sigma = 0, n = 1$. As has been shown in [5,6], the system

$$\dot{\rho} + \rho u_x = 0, \quad \rho \dot{u} + p_x = \gamma \rho, \quad \tau(\dot{p} - \chi \dot{\rho}) = \kappa \rho - p, \tag{4}$$

due to its symmetry properties [20], admits the ansatz

$$u = U(\omega) + D, \quad \rho = \rho_0 \exp(\xi t + S(\omega)), \quad p = \rho Z(\omega), \quad \omega = x - Dt, \tag{5}$$

where D is the constant velocity of wave front, ξ determines a slope of the inhomogeneity of the steady solution (5). According to [5], solutions (5) are described by the plane system of ODE which possesses limit cycles and homoclinic trajectories.

If we incorporate the second temporal derivatives in the last equation of system (3), then the previous DES is generalized to the following one:

$$\tau(\dot{p} - \chi \dot{\rho}) = \kappa \rho - p - h \left\{ \ddot{p} + \chi \left(\frac{2}{\rho} (\dot{\rho})^2 - \ddot{\rho} \right) \right\}. \tag{6}$$

This model takes into account the dynamics of internal relaxation processes in more detail. As has been shown in [7], wave solutions (5) are described by the system of ODE with three dimensional phase space. This system possesses the limit cycles undergoing the period doubling cascade, and the chaotic attractors.

Consider now the model with relaxation and spatial nonlocality

$$\tau(\dot{p} - \chi \dot{\rho}) = \kappa \rho - p + \sigma \left\{ p_{xx} + \frac{p_x \rho_x}{\rho} - \chi \left(\rho_{xx} - \frac{\rho_x^2}{\rho} \right) \right\}. \tag{7}$$

Solutions (5) satisfy the following dynamical system

$$\begin{aligned} U \frac{dU}{d\omega} &= UW, \quad U \frac{dZ}{d\omega} = \gamma U + \xi Z + W(Z - U^2), \\ U \frac{dW}{d\omega} &= \{U^2[\tau(\gamma U + \xi Z - WU^2) + \chi \tau W + Z - \kappa] \\ &+ \sigma[(\xi + W)(2U(\gamma - UW) + \chi W) + (UW)^2]\} [\sigma(\chi - U^2)]^{-1}. \end{aligned} \tag{8}$$

This system has the fixed point

$$U_0 = -D, \quad Z_0 = \frac{\kappa}{1 - 2\sigma(\xi/D)^2}, \quad W_0 = 0, \quad \gamma = \frac{\xi Z_0}{D} \tag{9}$$

which is the only one lying in the physical parameter range.

We start with analyzing the linearized at the fixed point (9) system (8) with the matrix \hat{M}

$$\hat{M} = \begin{pmatrix} 0 & 0 & -D \\ \gamma & \xi & Z_0 - D^2 \\ A & B & C \end{pmatrix},$$

where

$$\begin{aligned} A &= \frac{D\kappa\xi(2\xi\sigma - D^2\tau)}{Q\sigma(2\xi^2\sigma - D^2)}, \quad B = \frac{D^2(1 + \xi\tau)}{Q}, \quad Q = \sigma(\chi - D^2), \\ C &= Q^{-1} \left\{ \xi\sigma(\chi - D^2) - \frac{2D^2\kappa\xi\sigma}{D^2 - 2\xi^2\sigma} + D^2\tau(\chi - D^2) \right\}. \end{aligned}$$

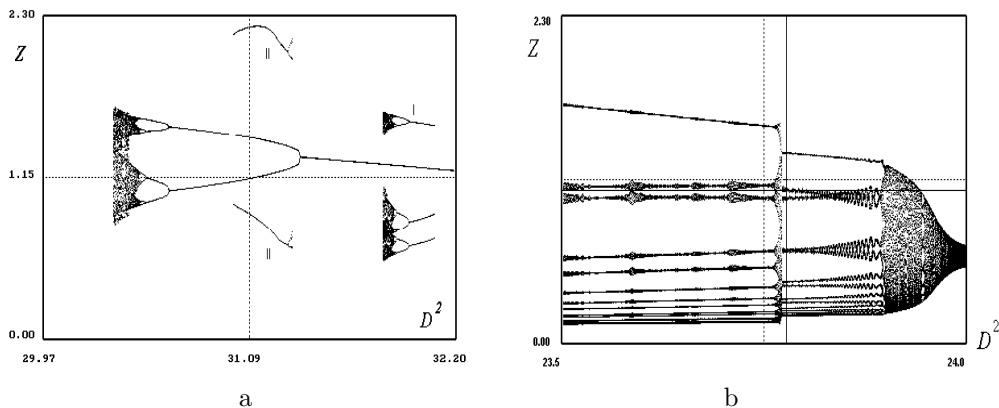


Figure 1: Bifurcation diagrams of system (8) in the plane (D^2, Z) obtained for $\chi = \eta = 50$, $\xi = 1.8$, $\tau = 0.1$, $\sigma = 0.76$ and $\kappa = 14$ (a), $\kappa = 1$ (b).

The well-known Andronov-Hopf bifurcation theorem [21] tells us that periodic solution creation can take place if the spectrum of matrix \hat{M} is $(-\alpha; \pm\Omega i)$. This is so if the following relations hold:

$$\alpha = \xi + C > 0, \quad (10)$$

$$\Omega^2 = AD - B(Z_0 - D^2) + \xi C > 0, \quad (11)$$

$$\alpha\Omega^2 = \xi(AD - Z_0B) > 0. \quad (12)$$

The first two take on the form of inequalities imposing some restrictions on the parameters. The third one determines the neutral stability curve (NSC) in the space $(D^2; \kappa)$ provided that the remaining parameters are fixed. For $\sigma = 0.76$, $\xi = 1.8$, $\tau = 0.1$, $\chi = 50$, it looks like a parabola with branches directed from left to right, see Figure 2a. Crossing the NSC from right to left, we observe the limit cycle appearance. Development of limit cycle at decreasing D^2 is convenient to study by means of the Poincaré section technique [13, 22].

Let us choose the plane $W = 0$ as an intersecting one and find coordinates of intersection points of phase curves which cross-section the intersecting plane only in one direction. Plotting coordinate Z of the cross-section point along the vertical axis, and the value of the bifurcation parameter D^2 along the horizontal one, we will obtain the typical bifurcation diagrams in (Figure 1). From the analysis of diagram Figure 1a we can see that while parameter D^2 decreases the development of the limit cycle coincides with the Feigenbaum scenario, followed by the creation of a chaotic attractor. Moreover, in the vicinity of the main limit cycle there are the hidden attractors (designated in Figure 1a by the symbols I and II). These attractors can be visualized by the integrating of system (8) with special initial data only.

In Figure 1b we see the torus development at decreasing D^2 . According to the diagram, we can distinguish tori with densely wound trajectories and striped tori.

Proceeding in the same way, we get the two-parameter bifurcation diagram (Figure 2) which shows that system (8) possesses the periodic, multiperiodic, quasiperiodic, and chaotic trajectories.

Such a complicated structure of the phase space of the system can be caused by

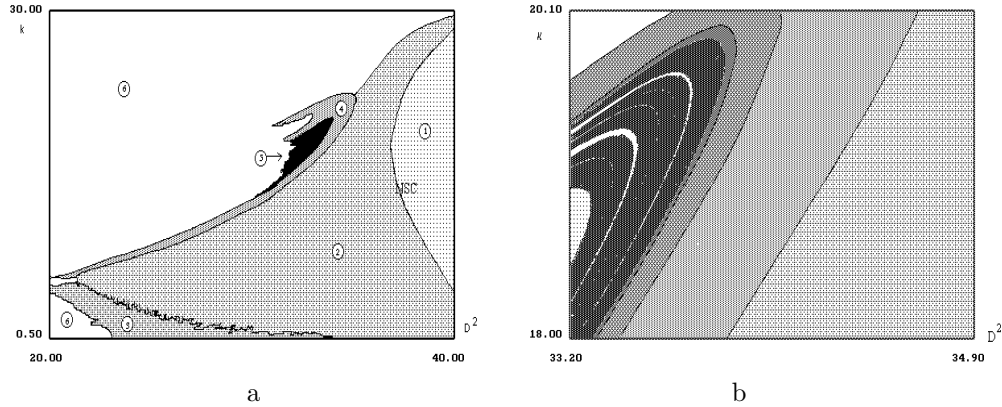


Figure 2: Left: bifurcation diagram of system (8) in parametric space (D^2, κ) : 1 – stable focus; 2 – $1T$ -cycle; 3 – torus; 4 – multiperiodic attractor; 5 – chaotic attractor; 6 – loss of stability. Right: enlargement of part of the left figure: 6 – $3T$ -cycle.

homoclinic trajectory existence.

3 Homoclinic Loops of Shilnikov Type and Their Bifurcations

It is worth noting that existence of homoclinic trajectories, i.e. loops consisting of the separatrix orbits of hyperbolic fixed point, plays a crucial role [16, 19] in the formation of localized regimes (solitary waves) in the phase space of dynamical system. It turned out that the incorporation of spatial nonlocality causes the creation of solitary waves with oscillating tails, whereas the well-known soliton equations have solutions with monotonic asymptotics or compact support (compactons) [17].

For the present, the problem on the existence of homoclinic trajectory of Shilnikov type [18, 21] in system (8) has been treated numerically.

We investigate a set of points of parameter space (D^2, κ) for which the trajectories moving out of the origin along the one-dimensional unstable invariant manifold W^u return to the origin along the two-dimensional stable invariant manifold W^s . In practice, for the given values of parameters κ, D^2 , we numerically define a distance (the counterpart of split function in [18], p. 198) between the origin and the point $(X^\Gamma(\omega), Y^\Gamma(\omega), W^\Gamma(\omega))$ of the phase trajectory $\Gamma(\cdot; \kappa, D^2)$:

$$f^\Gamma(\kappa, D^2; \omega) = \sqrt{[X^\Gamma(\omega)]^2 + [Y^\Gamma(\omega)]^2 + [W^\Gamma(\omega)]^2},$$

starting from the fixed Cauchy data $(0, 0, 0.001)$. Next we determine

$$\Phi(\kappa, D^2) = \min_{\omega} \{f^\Gamma\} \tag{13}$$

for the part of the trajectory which lies beyond the point at which the distance gains its first local maximum, providing that it still lies inside the ball centered at the origin and having a fixed (sufficiently large) radius (for this case $f^\Gamma(\omega) \leq 5$). The results are presented in Figure 3. The first one is of the most rough scale in this series. Here, white color marks the values of parameters κ, D^2 for which $\Phi > 1.2$, light grey corresponds to

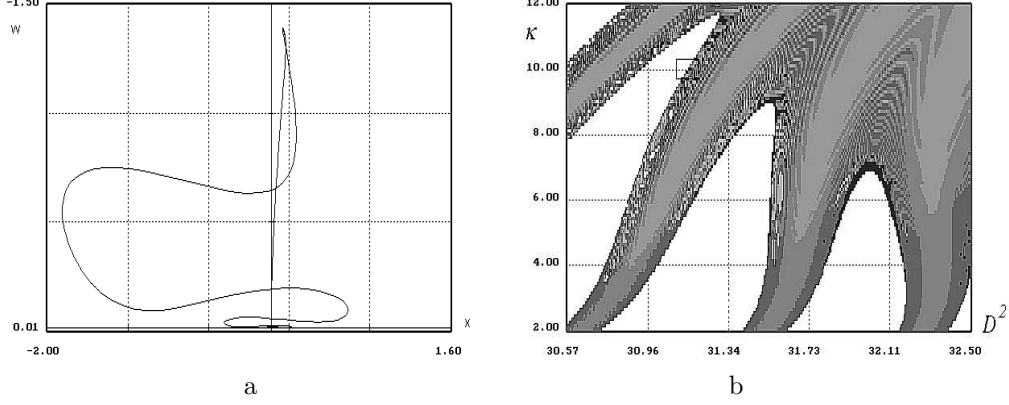


Figure 3: a) Projection of the homoclinic solution of system (8) onto the (X, W) plane. b) A portrait of subset of parameter space (D^2, κ) , corresponding to different intervals of function $f_{\min}^{\Gamma}(D^2, \kappa)$ values and the following Cauchy data: $X(0) = Y(0) = 0, W(0) = 0.001$: $f_{\min}^{\Gamma} > 1.2$ for white colour; $0.6 < f_{\min}^{\Gamma} \leq 1.2$ for light grey; $0.3 < f_{\min}^{\Gamma} \leq 0.6$ for grey; $0.01 < f_{\min}^{\Gamma} \leq 0.3$ for dark grey; $f_{\min}^{\Gamma} \leq 0.01$ for black.

the cases when $0.9 < \Phi < 1.2$ and so on (further explanations are given in the subsequent captions). The black coloured patches correspond to the case when $\Phi < 0.01$. In [11] the structure of the set of points in Figure 3b has been studied in more detail.

4 Models with DES taking spatial and temporal nonlocalities into account

Combining the models (6) and (7), we obtain the following spatio-temporal nonlocal model

$$\begin{aligned} \tau(\dot{p} - \chi\dot{\rho}) &= \kappa\rho - p + \sigma \left\{ p_{xx} + \frac{1}{\rho} p_x \rho_x - \eta \left(\rho_{xx} - \frac{\rho_x^2}{\rho} \right) \right\} \\ &\quad - h \left\{ \ddot{p} + \eta \left(\frac{2}{\rho} (\dot{\rho})^2 - \ddot{\rho} \right) \right\}. \end{aligned} \quad (14)$$

This model has been studied in [8,14], when the parameters h and σ are regarded as small quantities, i.e., equations (6) and (7) are perturbed by the terms with high derivatives. It turned out that the wave localized regimes are saved under perturbations and undergo some smooth changes.

5 Models Involving DES with the Third Temporal Derivatives

If we need to describe the relaxing processes in more detail, then we can incorporate the terms with the third temporal derivatives in DES (14). In such case DES has the form [3]

$$\begin{aligned} \tau(\dot{p} - \chi\dot{\rho}) &= \kappa\rho - p + \sigma \left\{ p_{xx} + \frac{1}{\rho} p_x \rho_x - \chi \left(\rho_{xx} - \frac{1}{\rho} (\rho_x)^2 \right) \right\} \\ &\quad - h \left\{ \ddot{p} + \chi \left(\frac{2}{\rho} (\dot{\rho})^2 - \ddot{\rho} \right) \right\} + \frac{h^2}{\tau} \ddot{p} + \frac{h^2 \chi}{\tau} \left\{ -\frac{6\dot{\rho}^3}{\rho^2} + \frac{6\dot{\rho}\ddot{\rho}}{\rho} - \ddot{\rho} \right\}. \end{aligned} \quad (15)$$

Solutions (5) satisfy the following dynamical system

$$\begin{aligned}
 U \frac{dU}{d\omega} &= UW, \quad U \frac{dZ}{d\omega} = \gamma U + \xi Z + W(Z - U^2), \quad U \frac{dW}{d\omega} = UR, \\
 U \frac{dR}{d\omega} &= (bU^3 (\chi - U^2))^{-1} \{-\kappa U^2 + \eta \xi \sigma W - 2\xi \sigma U^2 W + \chi \tau U^2 W - h \xi U^4 W \\
 &+ b \xi^2 U^4 W - \tau U^4 W + \eta \sigma W^2 + (\chi h - \sigma) U^2 W^2 - h U^4 W^2 + b \xi U^4 W^2 - b \chi U^2 W^3 \\
 &+ b U^4 W^3 + \gamma (2\xi \sigma U + h \xi U^3 - b \xi^2 U^3 + \tau U^3 + 2\sigma U W) + U^2 Z + h \xi^2 U^2 Z \\
 &- b \xi^3 U^2 Z + \xi \tau U^2 Z + (-\eta \sigma U + U^3 \{\sigma + \chi h - 4b \chi W - h U^2 + b \xi U^2 + 4b W U^2\}) R\},
 \end{aligned}
 \tag{16}$$

where $b = h^2/\tau$, and quadrature

$$U \frac{dS}{d\omega} = -(W + \xi).$$

The fixed point of this system has the coordinates

$$U_0 = -D, Z_0 = \frac{\kappa D^2}{D^2 - 2\sigma \xi^2}, W_0 = 0, R_0 = 0.
 \tag{17}$$

The conditions under which the linearized matrix

$$\hat{M} = \begin{pmatrix} 0 & 0 & a_1 & 0 \\ a_2 & a_3 & a_4 & 0 \\ 0 & 0 & 0 & a_5 \\ a_6 & a_7 & a_8 & a_9 \end{pmatrix} = \begin{pmatrix} 0 & 0 & -D & 0 \\ \gamma & \xi & Z_0 - D^2 & 0 \\ 0 & 0 & 0 & -D \\ a_6 & a_7 & a_8 & a_9 \end{pmatrix},
 \tag{18}$$

$$\begin{aligned}
 a_6 &= \frac{\kappa \xi (-2\xi \sigma + D^2 (h \xi - b \xi^2 + \tau))}{\Delta D (2\xi^2 \sigma - D^2)}, \quad a_7 = -\frac{1 + h \xi^2 - b \xi^3 + \xi \tau}{\Delta}, \\
 a_8 &= \frac{\xi \sigma (2Z_0 - \eta) + D^4 (h \xi - b \xi^2 + \tau) - D^2 (\chi \tau - 2\xi \sigma)}{D^2 \Delta}, \\
 a_9 &= \frac{\chi D^2 h - D^4 h + b D^4 \xi + D^2 \sigma - \eta \sigma}{D \Delta}, \quad \Delta = b D (\chi - D^2)
 \end{aligned}$$

admits the spectrum $(\pm \Omega^2 i; -\alpha_1; -\alpha_2)$ have the form

$$B_2 = \frac{B_1}{B_3} + B_0 \frac{B_3}{B_1}, \quad B_3^2 - 4B_0 \frac{B_3}{B_1} \geq 0,
 \tag{19}$$

where $B_3 = -a_3 - a_9$, $B_2 = a_3 a_9 - a_5 a_8$, $B_1 = a_5 (a_3 a_8 - a_1 a_6 - a_4 a_7)$, $B_0 = a_1 a_5 (a_3 a_6 - a_2 a_7)$ are the coefficients of characteristic polynomial for the matrix \hat{M} .

If we fix the parameters $\chi = \eta = 30$, $\xi = -1.9$, $h = 1$, $\tau = 1$, $b = 1$, $\sigma = 2.7$, then in the plane (D^2, κ) equation (19) defines the NSC. Crossing this curve at the point $A(2.2852; 3.7)$, one can observe the appearance of the limit cycle at $D^2 \geq 2.2852$.

In the Poincaré diagram depicted at increasing D^2 (Figure 4) we can identify the moments of several period doubling bifurcations leading to the chaotic attractor creation. But the chaotic attractor existing at a short interval of parameter D^2 is destroyed. Instead of it in the phase space of system (16) the complicated periodic trajectory in the shape of a loop (Figure 5a) appears.

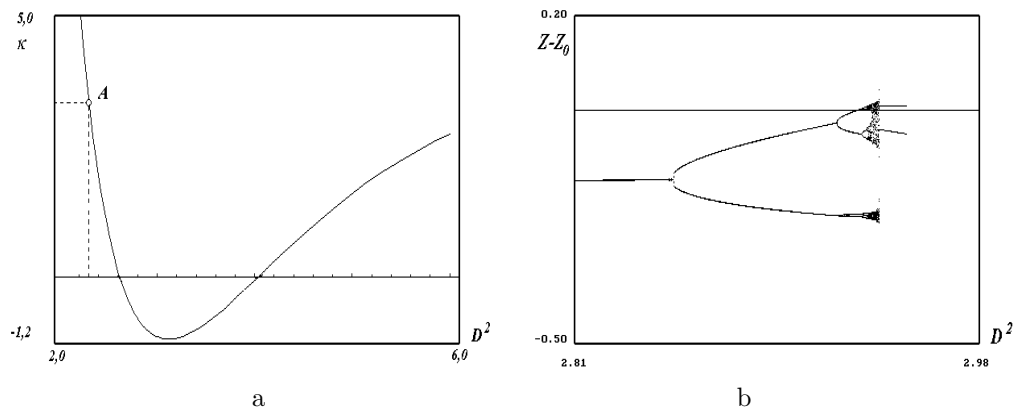


Figure 4: a) Neutral stability curve in the plane $(D^2; \kappa)$. b) The bifurcation Poincaré diagram at increasing D^2

Consider also the development of oscillating regimes whose basins of attraction are separated from the basin of attraction of the main limit cycle. Integrating dynamical system (16) from initial conditions $(0; 0; 0; 0.01)$ at $D^2 = 2.722$, we see that the phase space of the system, in addition to the main limit cycle, contains the complicated trajectory (Figure 5,a) which can be regarded as a hidden attractor. From the analysis of Poincaré diagram (Figure 6a) it follows that the system weakly responds to the growing of the parameter D^2 until $D^2 = 2.7445$. When $D^2 > 2.7445$, the system jumps to another type of oscillations followed by chaotic regime creation.

If we plot the Poincaré diagram at decreasing D^2 (Figure 6b) starting from the chaotic attractor, then we observe the periodic trajectory (Figure 5b) that differs from the initial regime (Figure 5a). Note that the periodic trajectory in Figure 5b can be revealed directly by the integration from the initial conditions $(0; 0; 0; 0.1)$.

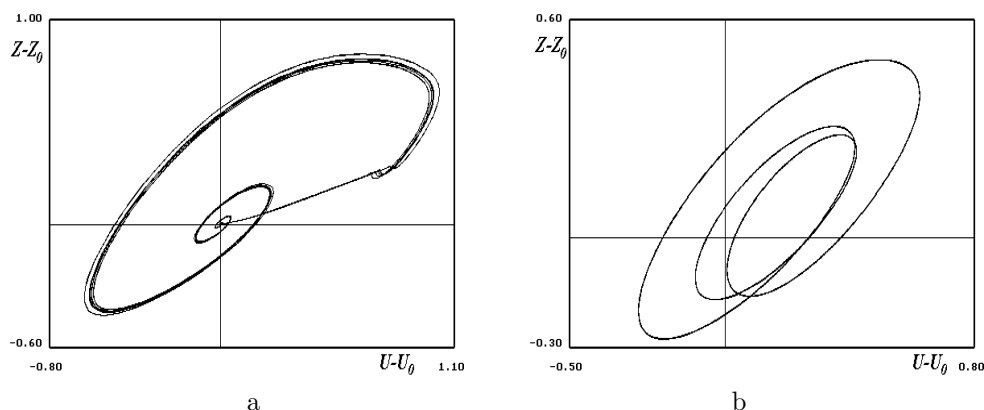


Figure 5: Phase portraits of separated trajectories derived at $D^2 = 2.722$, $\kappa = 3.7$, $b = 1$ and under different initial conditions.

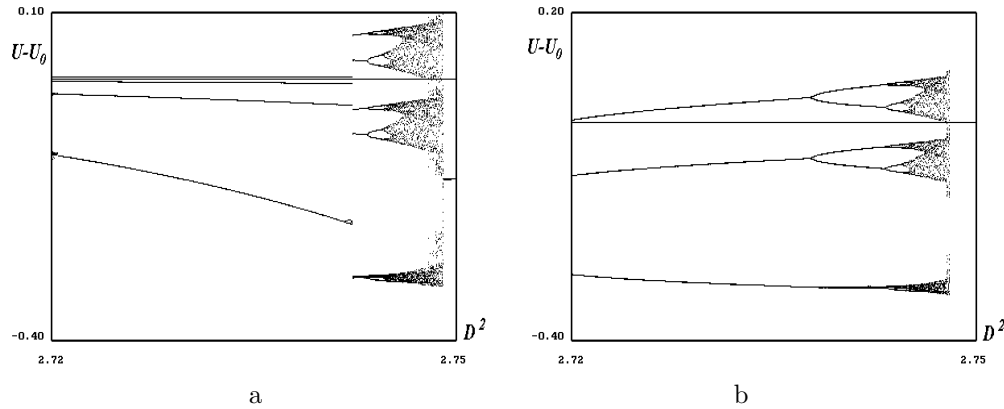


Figure 6: The bifurcation Poincaré diagram of development of separated regime at increasing D^2 (a) and decreasing D^2 . Here $b = 1$.

6 DES with Physical Nonlinearity and Second Derivatives

Till now we dealt with the models without physical nonlinearity. Generalizing the previous models in this direction, we obtain the following model [13]

$$\begin{aligned} & \sigma\chi\rho^{-2} [-\rho_{xx}(1+a) + \rho_x^2\rho^{-1}(1-na)] \\ & + h\chi\rho^{-2} [-\ddot{\rho}(1+a) + 2\dot{\rho}^2\rho^{-1}(1-0.5a(n-1)) \\ & + \tau h^{-1}\dot{\rho}(1+a)] + \kappa\rho^n = p + \tau\dot{p} - h\ddot{p} - \sigma(p_{xx} + \rho_x p_x \rho^{-1}), \quad a = \delta n \rho^{n+1}. \end{aligned} \tag{20}$$

Properties of solutions to system (20) can be found out using the symmetry of the system with respect to the Galilei group [20]. One can ascertain by direct verification that system (20) allows the operator

$$\hat{X} = \frac{1}{2\xi} \frac{\partial}{\partial t} + t \frac{\partial}{\partial x} + \frac{\partial}{\partial u}.$$

Let us construct an ansatz with its invariants

$$\rho = R(\omega), \quad p = P(\omega), \quad u = 2\xi t + U(\omega), \quad \omega = x - \xi t^2, \tag{21}$$

where parameter ξ is proportional to acceleration of the wave front. Substitution by (21) into the system yields the following quadrature

$$UR = C = \text{const}$$

and the dynamical system

$$\begin{aligned} R' &= W, \quad P' = \gamma R^m - 2\xi R + \frac{C^2}{R^2} W, \\ W' &= -(\kappa R^{n+3} - PR^3 - P'R^2 C\tau - hP'C^2 W \\ & + P'R^2\sigma W + \gamma m R^{2+m}\sigma W + \chi L\tau C W + \gamma h m R^m C^2 W \\ & + h\chi L(CWR^{-1})^2 - 2C^2\sigma W^2 + \chi M\sigma W^2 - 2C^4 h R^{-2} W^2 \\ & + 2h\chi N C^2 R^{-2} W^2 - 2R^3\sigma W\xi - 2hRC^2 W\xi) \times \\ & ((C^2 - \chi L)R(\sigma + hC^2 R^{-2}))^{-1}, \end{aligned} \tag{22}$$

where $(\cdot)' = \frac{d}{d\omega}(\cdot)$, $L = 1 + a$, $M = 1 - an$, $N = 1 - 0.5a(n - 1)$, $a = \delta n R^{n+1}$.

The single isolated equilibrium (neglecting the trivial) point has the following coordinates

$$R_0 = \left(\frac{2\xi}{\gamma}\right)^{1/m-1}, \quad P_0 = \kappa R_0^n, \quad W_0 = 0. \quad (23)$$

At this point the linearized matrix \hat{M} has the form

$$\hat{M} = \begin{pmatrix} 0 & 0 & 1 \\ a_1 & 0 & a_2 \\ a_3 & a_4 & a_5 \end{pmatrix}, \quad (24)$$

where

$$\begin{aligned} a_1 &= 2\xi(n-1), & a_2 &= C^2 R_0^{-2}, & a_4 &= R_0^2 \Delta^{-1}, \\ a_3 &= (2C^3 h [C^2 - \chi L] \tau [\gamma R_0^m - 2\xi R_0] R_0^{-2} \\ &\quad + C\chi(n+1)(L-1)\tau\Delta - C [C^2 - \chi L] \tau\Delta \\ &\quad - [C^2 - \chi L] (C^2 h R_0^{-2} + \sigma) \\ &\quad \times (\kappa n R_0^{1+n} - C\tau(\gamma(2+m)R_0^m - 6\xi R_0)))/\Delta^2, \\ a_5 &= (C^2 \gamma h (nR_0^n - R_0^m) - C^3 \tau + C\chi L\tau \\ &\quad + R_0^2 \sigma (\gamma [R_0^m + nR_0^n] - 4R_0 \xi))/R_0 \Delta, \\ \Delta &= (C^2 - \chi L) (C^2 h R_0^{-2} + \sigma). \end{aligned}$$

The NSC for system (22) has the following form

$$G(\xi, \sigma, n, h, \tau, \kappa, \chi) \equiv a_5 (a_3 + a_2 a_4) + a_1 a_4 = 0. \quad (25)$$

Let us make the values of parameters fixed as follows:

$$\begin{aligned} \gamma &= 1, & \chi &= 10, & C &= -2.8, & \sigma &= 0.2, \\ \tau &= 1.1, & h &= 3.2, & \delta &= 1.4, & n &= m = 3.2. \end{aligned}$$

Condition (25) allows us to find numerically the value of $\xi_0 = 0.157$ corresponding to birth of the limit cycle.

Let us consider in more detail the influence on the revealed regimes of parameters n and δ changes, which determine nonlinearity of the medium in the dynamic equation of state. Let us make the value of parameter $\xi = 0.35$ fixed, then there is a limit cycle with period $2T$ in the space of the system, and we construct the bifurcation diagram presented in Figure 7a.

The diagram reveals some peculiarities of system (22) behaviour. In particular, we would like to pay attention to the presence of a "special" point in the parameter plane surrounded by four different types of solutions. One can also see the "windows" of periodicity (area 6) in the chaotic area. To find out the structure of phase space in more detail near area 6, one-parametric Poincaré diagrams were plotted [13].

It turns out that abrupt reconstruction of the chaotic attractor structure can be observed, which is probably caused by the interaction of two (or more) co-existing attractors of the dynamic system. We also reveal that the chaotic trajectory is localized in a more

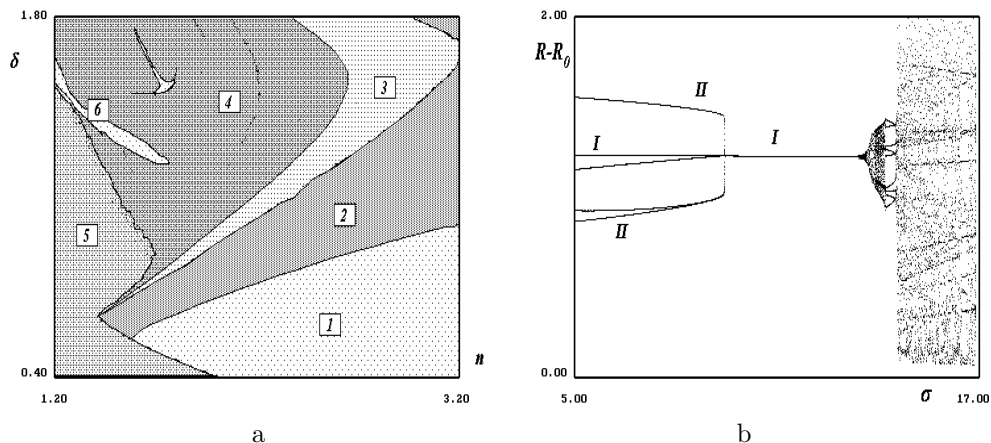


Figure 7: a) The two-parametric bifurcation diagram in case of $\gamma = 1$, $\chi = 10$, $C = -2.8$, $\tau = 1.1$, $\sigma = 0.2$, $\kappa = 0.9$, $h = 3.2$, $\xi = 0.35$, $m = 3.2$; b) The Poincaré bifurcation diagram for development of the torus in case of $\delta = 0.4$, $n = 3.2$ (for other values of parameters see Figure 7a) and increasing σ , where graph I is the basic limit cycle, graph II – complicated periodic trajectory with separated region of attraction.

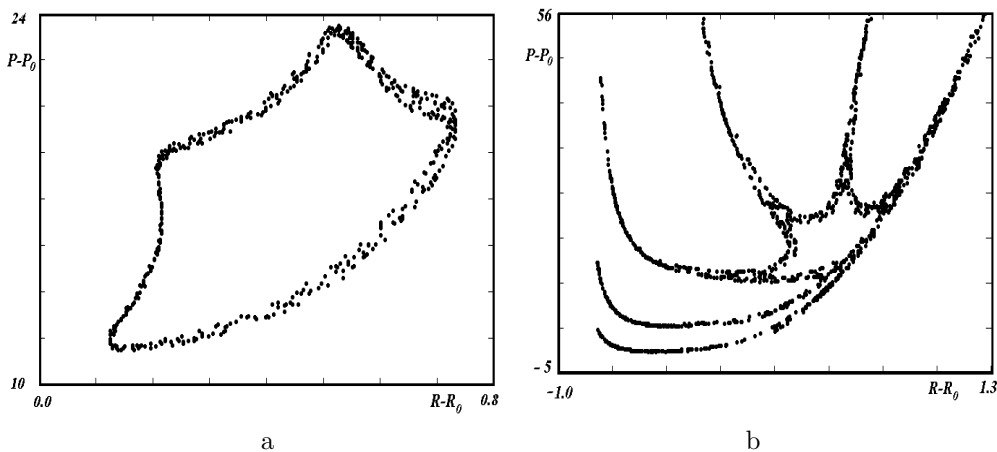


Figure 8: a) The Poincaré cross-section of the torus surface in case of $\sigma = 14$ b) The Poincaré cross-section of the chaotic attractor in case of $\sigma = 14.6$. Fixed parameters $\gamma = 1$, $\chi = 10$, $C = -2.8$, $\tau = 1.1$, $\kappa = 0.9$, $h = 3.2$, $\delta = 0.4$, $\xi = 0.35$, $n = m = 3.2$.

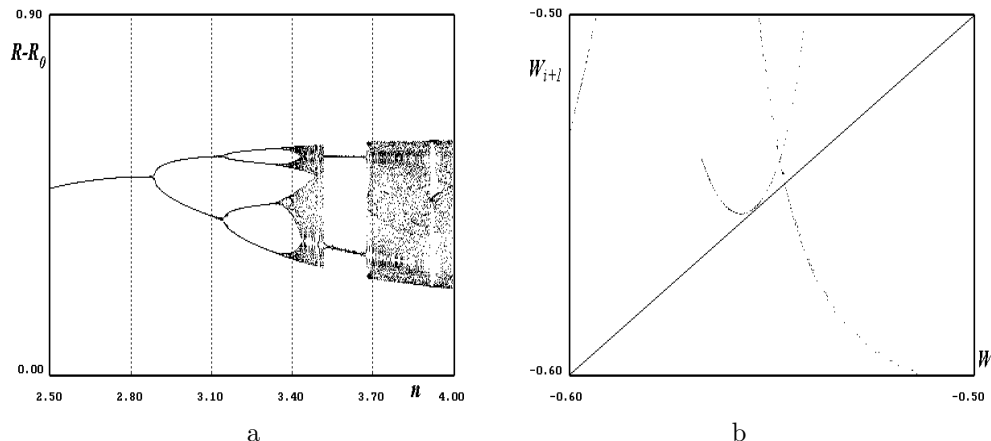


Figure 9: a) The bifurcation diagram at increasing n . b) The graph of dependence W_{i+1} vs W_i at $n = 4.25$. The fixed values of parameters $\gamma = 1.49$, $\chi = 50$, $C = -1.5$, $\tau = 0.1$, $\kappa = 1.9$, $\sigma = 0.2$, $h = 0.9$, $\xi = 0.18$, $\delta = 0.8$.

narrow area of phase space of system (22), stipulating the appearance of a specific window (area 6) of periodicity with a decrease of n . Analysis of two-parametric bifurcation diagrams for $\kappa > 0.9$ shows that the area of existence of chaotic attractors increases and the windows of regular behaviour in case of the increasing κ are shifted towards higher values of the nonlinearity parameter n .

A crucially different set of bifurcations is observed in case of a change of parameter σ .

Let us fix the values of parameters $\gamma = 1$, $\chi = 10$, $C = -2.8$, $\tau = 1.1$, $\kappa = 0.9$, $h = 3.2$, $\xi = 0.35$, $n = m = 3.2$ and $\delta = 0.4$. Integrating system (22) with the initial data $(0, 0, 0.01)$ and $\sigma = 5$ within phase space near the equilibrium point, in addition to the limit cycle, other periodic trajectory has been found with a separated pool of attraction (development of this regime with increasing of σ is presented in Figure 7b graph II).

The presence of such a regime leads to the assumption on the existence of quasi-periodic regimes. To look for such a regime let us plot a bifurcation diagram of Poincaré for development of basic limit cycle in case of increasing parameter σ (Figure 7b graph I).

Another bifurcation, leading to the appearance of the toroidal surface, has been discovered in this system. An intersection of the toroidal attractor with the plane $y_3 = 0$ forms a closed curve, shown in Figure 8a. A further increase of parameter σ causes the synchronization of tore frequencies, and finally an abrupt increase of vibrations amplitude, which shows the creation of a crucial new dynamical behavior. To clarify the character of the produced regime, let us analyze the Poincaré section for the case of $\sigma = 14.6$ (Figure 8b). The plotted cross-section is specific for chaotic attractor, which provides reasons for statements on the existence of bifurcation of a quasi-periodic regime with a producing chaotic attractor.

It turned out that system (22) provides another type of chaotic attractor creation, namely, intermittency. Let us fix $\gamma = 1$, $\chi = 50$, $C = -1.5$, $\tau = 0.1$, $\kappa = 1.9$, $\sigma = 0.2$, $h = 0.9$, $\xi = 0.18$.

Plotting the Poincaré bifurcation diagram (Figure 9a), we see that a limit cycle

undergoes several period doubling bifurcations resulting in the chaotic attractor creation. But the development of chaotic attractor is interrupted suddenly and new complicated periodic trajectory appears which bifurcates in chaotic attractor as well at increasing n . Considering the hereditary sequences (Figure 9b) for chaotic trajectories, we found that the graph of the map $W_{i+1} = f(W_i)$ is close to the bissectrice at $n = 4.25$. As in the case with the Lorentz system, existence of narrow passage leads to the alternation of the chaotic and regular behavior of the system trajectories.

7 Conclusions

Finally, we have studied the hierarchical sequences of the mathematical models for non-equilibrium media. Analyzing the wave fields in such media we have shown that the derived models possess wide set of localized wave regimes. In particular, the models with relaxation admit periodic, multiperiodic and chaotic solutions. Spatially nonlocal models have in addition quasiperiodic and solitary wave solutions. All the models demonstrate most bifurcations and scenarios of chaotic regimes creation. The equations of state utilized in this paper are suitable for developing other models of complicated nonequilibrium systems [23].

On the other hand, identifying internal variables with parameters undergoing fluctuations, one can consider these investigations as the problem on the dissipative structures creation under the influence of noise.

References

- [1] Vladimirov, V.A., Danylenko, V.A. and Korolevych, V.Yu. Nonlinear models for multi-component relaxing media: dynamics of wave structures and qualitative analysis. Subbotin Institute of Geophysics, Prepr., Kyiv, 1990.
- [2] Danevych, T.B. and Danylenko, V.A. Governing equations for nonlinear media with internal variables taking temporal and spatial nonlocalities into account. Subbotin Institute of Geophysics, Prepr., Kyiv, 1999.
- [3] Danevych, T.B., Danylenko, V.A. and Skurativskyi, S.I. Nonlinear Mathematical Models of Media with Temporal and Spatial Nonlocalities. Subbotin Institute of Geophysics, Kyiv, 2008. [Ukrainian]
- [4] De Groot, S.R. and Mazur, P. *Nonequilibrium Thermodynamics*. Amsterdam, North-Holland, 1962.
- [5] Vladimirov, V.A. Classical and generalized invariant solutions of the relaxing hydrodynamics equations. *Opuscula Mathematica* **23** (2003) 81–94.
- [6] Danylenko, V.A., Sorokina, V.V. and Vladimirov, V.A. On the governing equations in relaxing media models and self-similar quasiperiodic solutions. *J. Phys. A: Math. Gen.* **26** (1993) 7125–7135.
- [7] Sidorets, V.N. and Vladimirov, V.A. On the peculiarities of stochastic invariant solutions of a hydrodynamic system accounting for non-local effects. In: *Symmetry in Nonlinear Mathematical Physics*, Vol. 2. Institute of Mathematics, Kyiv, 1997, 409–417.
- [8] Vladimirov V., A., Danylenko, V.A. and Skurativskyi, S.I. Quasiperiodic and chaotic solutions of the nonlocal model of a multicomponent medium. *Reports of the NAS of Ukraine* **12** (2004) 104–108.
- [9] Danylenko, V.A. and Skurativskyi, S.I. Chaotic invariant solutions of nonlinear nonlocal models for multicomponent media with internal oscillators. *Reports of the NAS of Ukraine* **9** (2006) 111–115.

- [10] Vladimirov, V.A., Sidorets, V.N. and Skurativskyi, S.I. Complicated travelling wave solutions of a modelling system describing media with memory and spatial nonlocality. *Rep. Math. Phys.* **44**(1/2) (1999) 275–282.
- [11] Vladimirov, V.A. and Skurativskyi, S.I. Soliton-like solutions and other wave patterns in the nonlocal model of structured media. *Rep. Math. Phys.* **46** (2000) 287–294.
- [12] Vladimirov, V.A. and Skurativskyi, S.I. Investigations of the autowave solutions of a model of structured media with spatial and temporal nonlocality. *Rep. Math. Phys.* **49** (2002) 405–414.
- [13] Danylenko, V.A. and Skurativskyi, S.I. Invariant chaotic and quasi-periodic solutions of nonlinear nonlocal models of relaxing media. *Rep. Math. Phys.* **59** (2007) 45–51.
- [14] Skurativskyi, S.I. On the autowave solutions of some model of structured media accounting for effects of spatio-temporal nonlocality. *Nonlinear Phenom. Complex Syst.* **4**(4) (2001) 390–396.
- [15] Danylenko, V.A. and Skurativskyi, S.I. Soliton-like waves in nonequilibrium media. *Reports of the NAS of Ukraine* **10** (2012) 96 – 102.
- [16] Wiggins, S. *Introduction to Applied Nonlinear Dynamical Systems and Chaos*. Springer-Verlag, New York, 1990.
- [17] Wazwaz, A-M. Peakons and soliton solutions of newly developed Benjamin-Bona-Mahony-like equations. *Nonlinear Dynamics and Systems Theory* **15** (2) (2015) 209–220.
- [18] Kuznetsov, Yu.A. *Elements of Applied Bifurcation Theory*. Springer-Verlag, New York, 1998.
- [19] Butenin, N.V., Neimark, J.I. and Fufaev, N.A. *Introduction to the Theory of Nonlinear Oscillations*. Moscow, Nauka, 1987. [Russian]
- [20] Lahno, V.I., Spichak, S.V. and Stogniy, V.I. *Symmetry Analysis of Evolution Type Equations*. Moscow–Igevsik, Computer Research Institute, 2004. [Russian]
- [21] Guckenheimer, J. and Holmes, P. *Nonlinear Oscillations, Dynamical Systems and Bifurcations of Vector Fields*. New York, Springer-Verlag, 1987.
- [22] Holodniok, M., Klić, A., Kubiček, M. and Marek M. *Methods of Analysis of Nonlinear Dynamical Models*. Moscow, World Publishing House, 1991. [Russian]
- [23] Danylenko, V.A. and Skurativskyi, S.I. Travelling wave solutions of nonlocal models for media with oscillating inclusions. *Nonlinear Dynamics and Systems Theory* **12**(4) (2012) 365–374.